This project has received funding from the European Union's Seventh Programme for research, technological development and demonstration under grant agreement No [308417]".

New Directions in Seismic Hazard Assessment through Focused Earth Observation in the Marmara Supersite

Grant Agreement Number: 308417
co-funded by the European Commission within the Seventh Framework Programme
THEME [ENV.2012.6.4-2]
[Long-term monitoring experiment in geologically active regions of Europe prone to natural hazards: the Supersite concept]

D4.4

Report on the high-resolution monitoring and analysis of the seismicity and velocity perturbations

Project Start Date	1 November 2012
Project Duration	36 months
Project Coordinator /Organization	Nurcan Meral Özel / KOERI
Work Package Number	4
Deliverable Name/ Number	Report on the high-resolution monitoring and analysis of the seismicity and velocity perturbations/D 4.4
Due Date Of Deliverable	30/4/2016
Actual Submission Date	30/4/2016
Organization/Author (s)	CNRS/Michel Bouchon

Dissemination Level		
PU	Public	
PP	Restricted to other programme participants (including the Commission)	
RE	Restricted to a group specified by the consortium (including the Commission)	
CO	Confidential, only for members of the consortium (including the Commission)	

TABLE OF CONTENTS

1. SEISMIC VELOCITY PERTURBATIONS FROM SEISMIC NOISE CORRELATION

1.1 AMBIANT NOISE TOMOGRAPHY AROUND THE MARMARA SEA

Surface waves contain a great deal of information on the structure of the Earth's crust and upper mantle. The large amplitudes with relatively low attenuation and long propagation paths provide significant contribution to the knowledge of the earth models. At different periods they are sensitive to the different depths. In general, short periods tend to sample the slower and shallow layers, while the long periods are sensitive to faster velocities and deeper layers. Measurements made from earthquake-based surface waves, however, have some limitations; e.g, inadequate path coverage due to the inhomogeneous distribution of sources, dependency on origin time and source parameters.

Recently, it has been shown that a random wavefield generated by scatters in the near-surface structure of the Earth, the Green's function between two points can be estimated from the cross-correlation of recordings made at the two locations over sufficiently long times Observations of diffuse seismic wavefields overcome some of the problems affecting traditional surface wave measurements made on earthquake recordings. We have analyzed continuous broadband vertical-component seismic data spanning the period from 2008 to 2014 recorded by 121 stations in the in the Marmara Sea region (Figure 1). The use of vertical-component data limits the analysis to Rayleigh waves. A continuous waveform database was created for the analysis prior to cross-correlation. Data from the stations were sampled to 5 sps and processed one day at a time in single-station and station-pairs. Mean, trend, and instrument response were removed. Earthquakes and other disturbing effects such as instrumental irregularities were also removed by applying temporal normalization. Additionally, spectral whitening was applied in order to reduce the effects of primary (~14 sec) and secondary (~7 sec) microseism. In general, data processing procedure was similar to the one described in the work of Bensen et al. (2007).

After the cross-correlations were computed and stacked, the resulting waveform gives an estimated Green's function between two receivers. The Green's functions with the inter-station distance smaller than 3 wavelength ($\Delta > 3\lambda$) were discarded. Group velocities as a function of period are obtained by applying a frequency–time analysis technique (Dziewonski et al., 1969). The Rayleigh wave dispersion measurements are then used to obtain the group velocity maps at periods from 6 to 20 s on a $0.1^\circ \times 0.1^\circ$ grid spanning Marmara Sea and the surrounding region, using the tomographic method presented by Cambaz and Karabulut (2010).

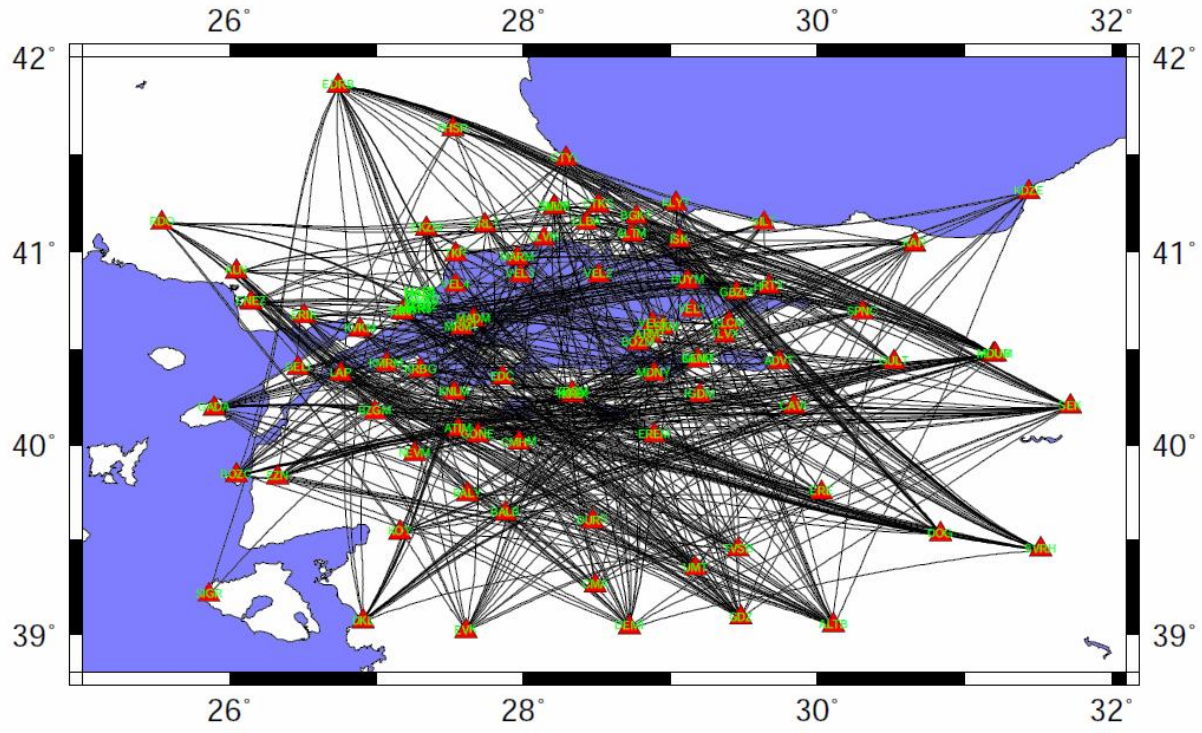

Figure 1: Seismic stations (red triangles) used for the noise correlation tomography in the Marmara.

1.2 GROUP VELOCITY MAPS

Figure 2 shows the group velocity maps at a period of 10 secs. The velocity perturbations are displayed as deviations from the average velocity at the computed period (2.70km/s). Lower velocities are presented as red and higher velocity as blue on the maps. A variety of geological features are recognizable in the estimated group velocity dispersion maps. The dispersion map displays low group speeds for the sedimentary basins in the Marmara Sea and the Thrace basin. The higher velocities are observed on the north, within the Istanbul Zone and Rhodope massif. Figure 3 is a regional geological map from Lepichon et al, 2014 for comparison. The velocity contrast across the MMF is apparent. The Thrace basin also appears with a large low velocity anomaly bounded by the high velocities of the Pontides on the north.

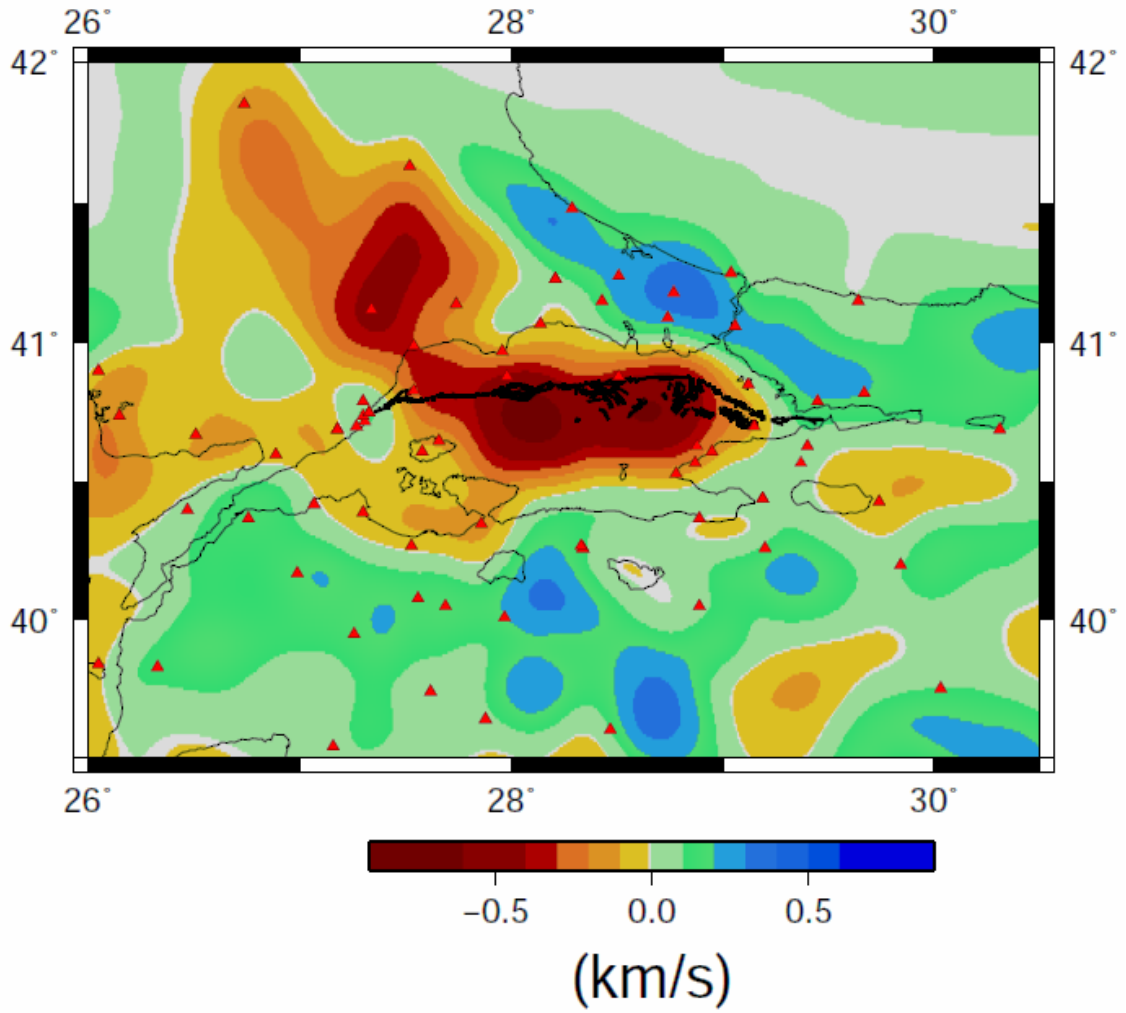

Figure 2: Group velocity map at 10sec period. The velocity variations are displayed as perturbations from 2.70 km/s. The red triangles show the stations used for the computations.

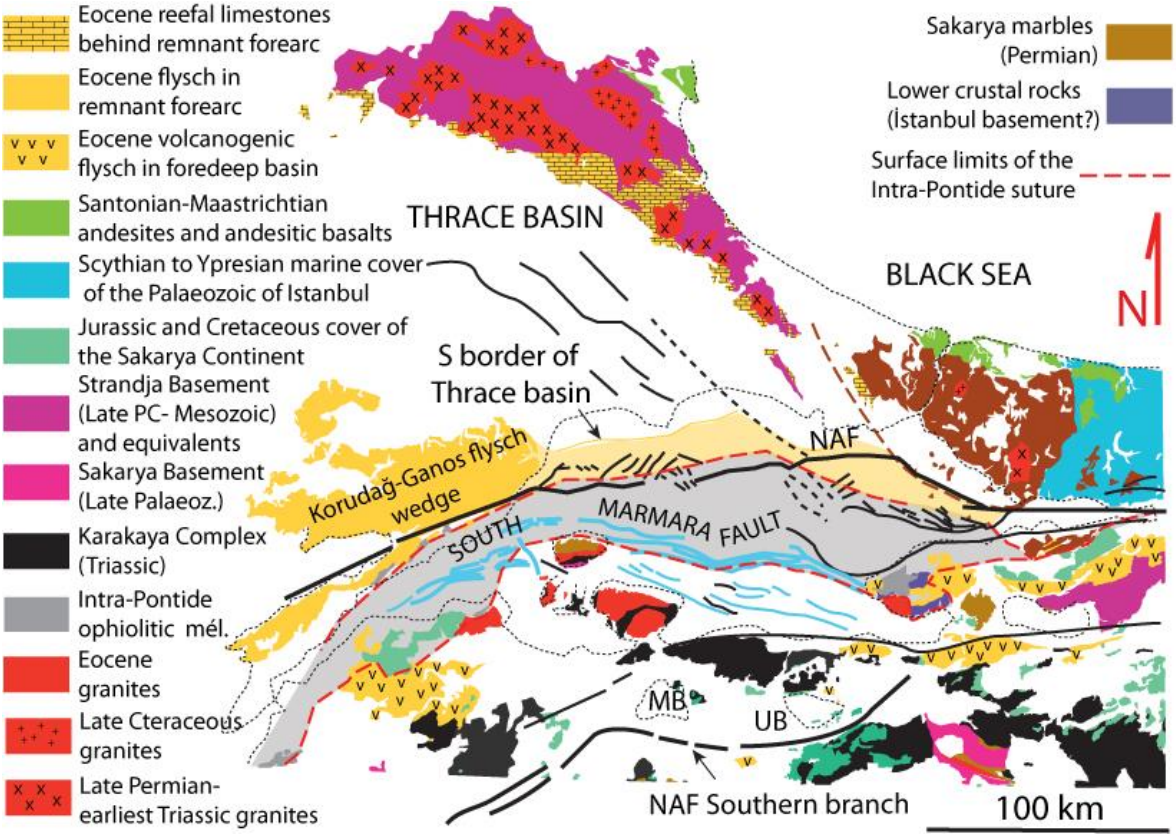

Figure 3: A schematic map showing the tectonic features of the Marmara region. Black lines are mid-Miocene to younger right- lateral strike-slip faults. Blue lines mark the location of the faults belonging to the South Marmara Fault. The northern branch of the North Antolian Fault closely follows the contact between the Paleozoic of Istanbul and the Sakarya basement and then jumps to follow the northern boundary of the Intra-Pontide suture (Le Pichon et al., 2014).

1.3 MONITORING OF VELOCITY CHANGES FROM NOISE CORRELATION

The Green's functions retrieved from ambient seismic noise records over different time periods are not stationary, and the temporal variations contain useful information. As the coda waves are scattered waves that travel long distances and accumulating the time delays as a consequence, measuring travel time perturbations in the coda allows detecting very small velocity changes. By exploring these temporal variations, it is possible to detect small velocity perturbations in the earth.

We analyzed 5 year of continuous seismic records from broad-band stations in the Marmara region. Using correlations of ambient seismic noise, relative velocity variations in the order of 0.05% are measured between the interstation pairs. We perform these measurements using the 'stretching' technique, assuming that one of two waveforms is a stretched version of the other. Between most of the interstation pairs in the area, a seasonal signal is observed, with peaks and troughs during winter and summer times, respectively.

Figure 4 shows the 15 day stacked Green's function between the station located in the Marmara Island (MADM) and the second station is located to the north on the other side of the Marmara sea in

Tekirdağ (TKR) . The path between two stations crosses the Main Marmara Fault in a region of high seismicity rate. An earthquake of Mw=5.2 occurred on the fault at 07.25.2011 is also located on the path. We used the continuous seismic data between January 2008 and December 2011. However there were significant gaps and timing errors in the data. The data were divided into 1-day (24 h) segments and resampled by 0.2s. We used the spectral band between 0.1 and 1.0 Hz. The cross-correlation functions are obtained by stacking 15 days of seismic noise. A reference Green functions is computed from the stacking of the Green functions for 15 day stacking. The temporal evolution was then tracked by comparing the reference Green functions with the 15 day stacked Green functions.

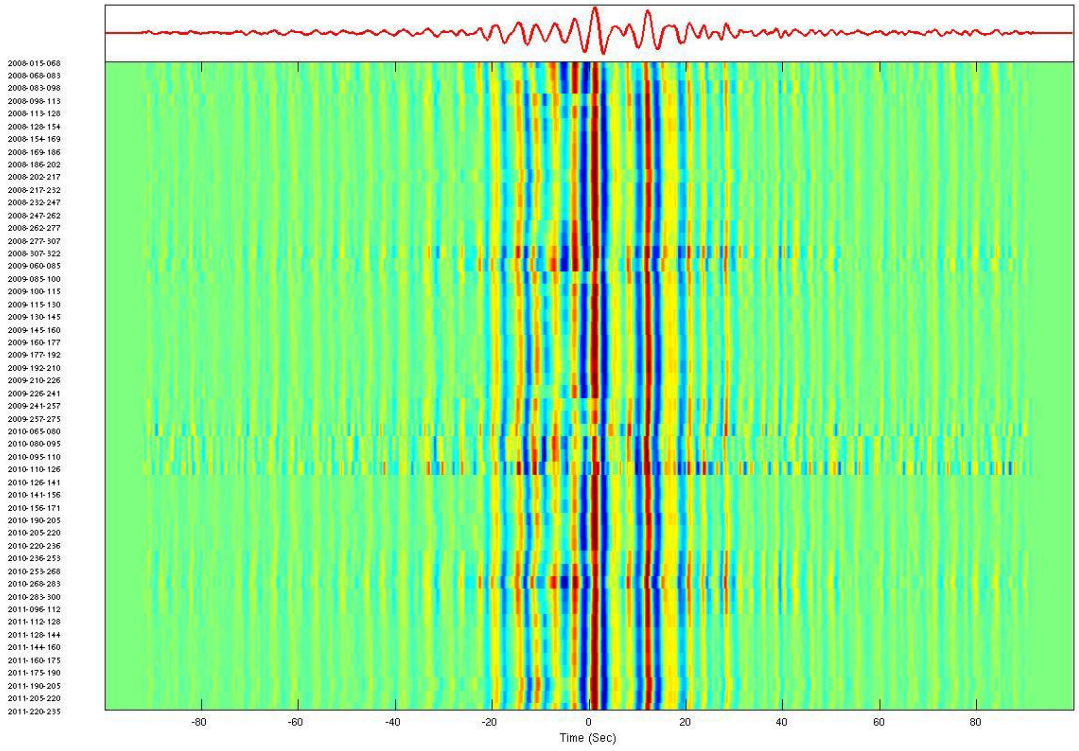

Figure 4: 15-day stacked cross-correlation functions (CCF) for receiver pair MADM-TKR. The red curve on the top of the figure represents the reference stacked cross correlation function. The CCFs are filtered between 0.1 and 1.0 Hz and normalized in amplitude. The numbers on the left shows the time period for the Green function computed.

Figure 5 shows the variations in the stretching factors computed from the 15 day stacked Green functions and reference Green functions. The ε= Δv/v is varying between -0.01 and 0.01 periodically. The perturbations are found to be correlated with the seasonal variations and no velocity perturbation is detected along the path between MADM and TKR stations.

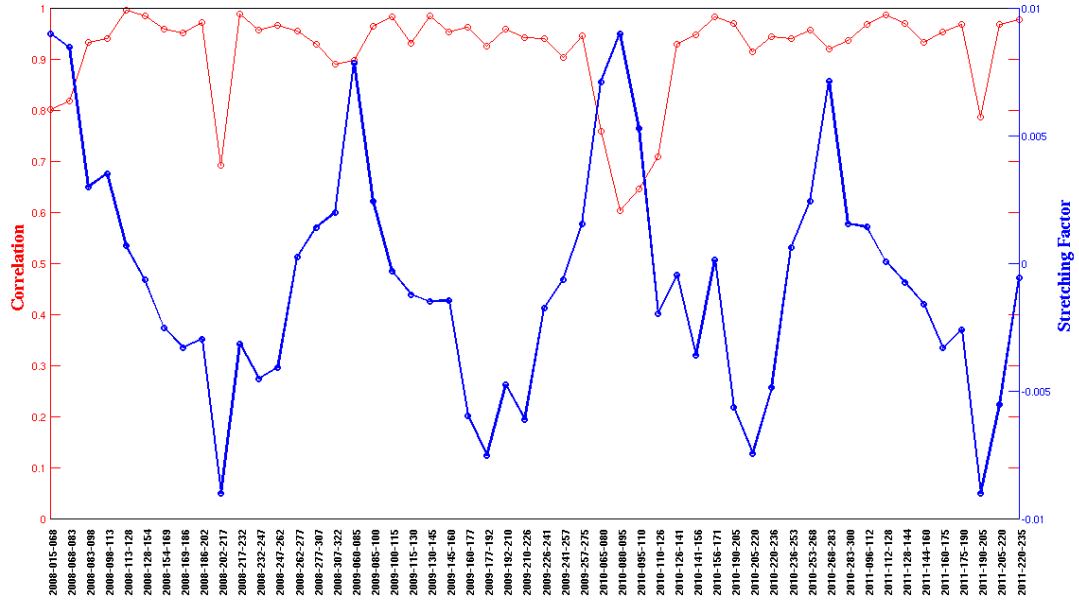

Figure 5: Measurements of relative velocity perturbations. Time shifts measured between the reference and 15 days stacked Green functions of Figure 4.

2 HIGH RESOLUTION MONITORING OF SEISMICITY IN THE MARMARA REGION

2.1 DATA ANALYSIS

The objective of the present study is to provide a high resolution analysis of the seismicity distribution along the MMF during the 2007-2012 period and to link it to geodetic observations. We first identify domains along the fault with coherent behaviors. We show the extent of the seismogenic zone both in time and space and compare it to the geodetic locking depth. We study the lateral variations of statistical properties of micro-seismicity: background seismic rate, b-values, seismic slip distribution. We identify swarms that might host the nucleation of the next major event or mark the barriers to large earthquake ruptures. We discuss the present seismo-tectonic behavior of the MMF.

We used seismic waveform data that were acquired between 2007 and 2012. The data were compiled from 132 seismic stations belonging to local permanent and temporary networks. The map of the seismic stations used for this study is shown in Fig. 6. It includes broadband stations operated by KOERI (Kandilli Observatory and Earthquake Research Institute) and MAM-TUBITAK (the scientific and technological research council of Turkey), the short period CINNET stations supported by ANR (the French national research agency), stations installed during the REAKT project by KOERI, the permanent cabled KOERI OBS stations, and the temporary OBS stations from IFREMER (French research institute for exploitation of the sea). The starting date of 2007 was chosen because of the increase of the station density around the Cinarcik basin at that period.

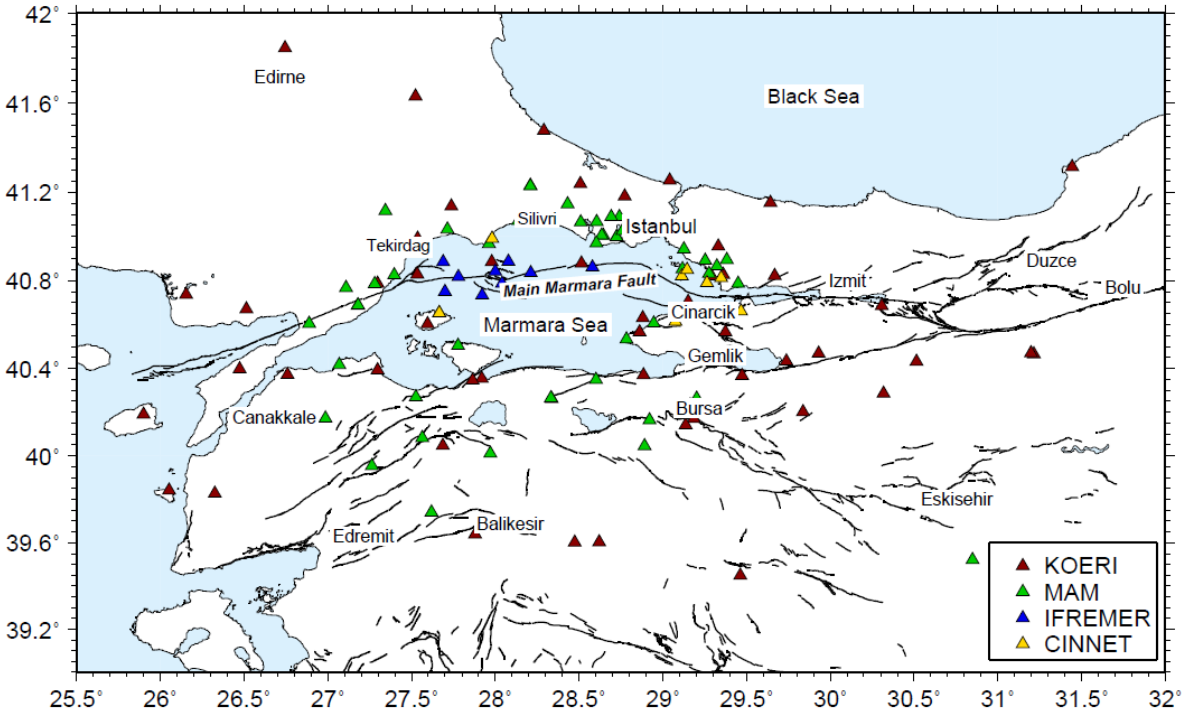

Figure 6: Map of 124 (out of the 132) seismic stations around the Marmara Sea used for this study from two permanent networks (KOERI and MAM) and two temporary networks (IFREMER and CINNET). The 8 stations used and not shown are on the south of this zone.

2.2 PRECISE LOCATION MAP

Detection windows have been obtained from a STA/LTA procedure. We manually picked P and S wave arrivals on all detection windows for which we could identify a clear phase arrival. The earthquake location has been performed from the SEISAN, HYPOCENTER program assuming a 1D velocity model. In order to improve the absolute location of the earthquakes, stations delays are also estimated from the VELEST software and introduced in the location.

The location procedure has been performed independently for two separate regions of the MMF but using the same velocity model. The first region comprises the eastern part of the Marmara Sea. It includes the Cinarcik basin and extends westward to the Istanbul area. In this region, we located 3092 events with a mean rms error of 0.09s. The second area comprises the western Marmara Sea and overlaps with the other region at the longitude of the city of Istanbul. In this area we located 1489 events with a mean rms error of 0.12s. Numerous events from quarry blasts have been removed as being shallow daily clusters of events. The obtained earthquake catalog for the whole Marmara region consists of 4581 events. It includes 1936 events along the MMF zone defined as a roughly 10 km thick region around the fault trace (the zone is broader to the west in the Tekirdag domain where secondary sub-parallel faults to the MMF exist). Typical absolute errors in longitude, latitude and depth are: 1km, 1km and 3km, respectively. Figure 7 shows the geographical and depth distribution of the seismicity.

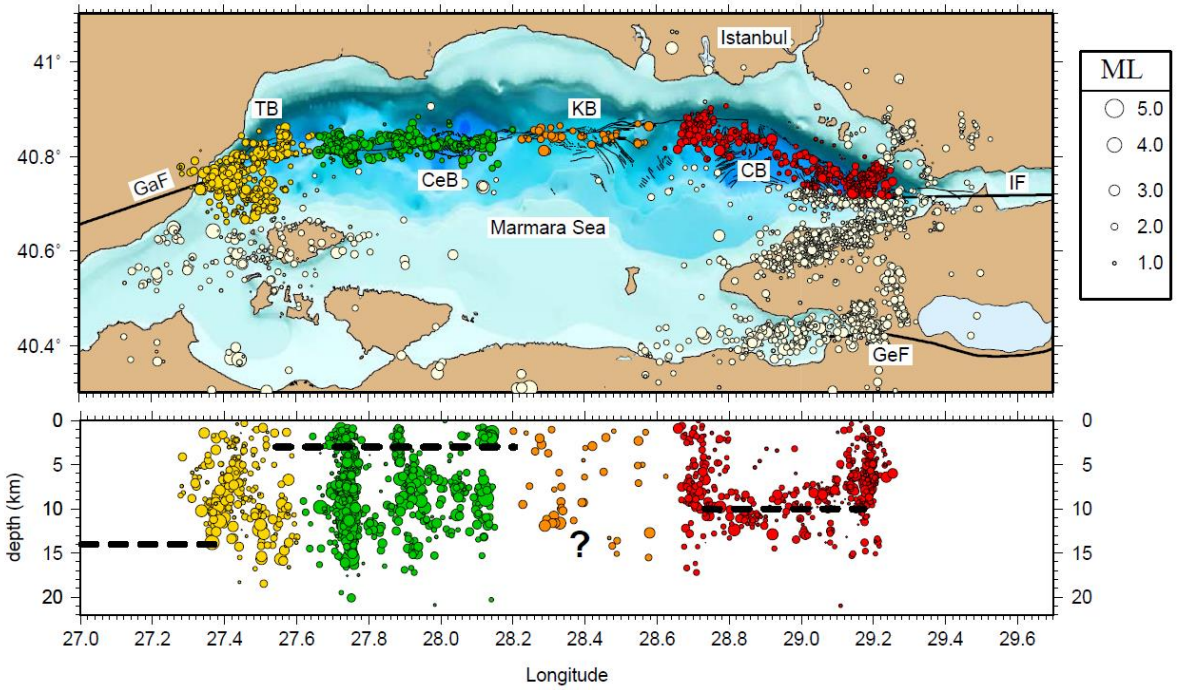

Figure 7: Map (top) and cross section (below) of the seismicity along the Main Marmara Fault during the period 2007-2012. Four domains are introduced: The Tekirdag basin (TB) in yellow, the Central basin (CeB) in green, the Kumburgaz basin (KB) in orange, and the Cinarcik basin (CB) in red. All the regional seismicity away from the MMF is plotted in white. Fault network:GaF for Ganos fault, IF for Izmit fault, GeF for Gemlik fault. Dotted lines in the depth section show the geodetically estimated locking depth of each domain.

Figure 7: Map (top) and cross section (below) of the seismicity along the Main Marmara Fault during the period 2007-2012. Four domains are introduced: The Tekirdag basin (TB) in yellow, the Central basin (CeB) in green, the Kumburgaz basin (KB) in orange, and the Cinarcik basin (CB) in red. All the regional seismicity away from the MMF is plotted in white. Fault network:GaF for Ganos fault, IF for Izmit fault, GeF for Gemlik fault. Dotted lines in the depth section show the geodetically estimated locking depth of each domain.

Based on the geographical and depth distribution of micro-seismicity between 2007 and 2012, four segments are defined along the MMF (see Fig 7) corresponding to the four major basins of the Marmara Sea. To the west, in the Tekirdag basin (TB) and Central Basin (CeB), seismicity is abundant and distributed over a wide depth range (from surface to 17 km). At the transition between TB and CeB (see Fig. 7 at longitude 27.74° corresponding to the Western High) we observe numerous earthquakes along a very extended cluster in depth. They are possibly related to fault offsets.

To the east, in the Cinarcik basin (CB), seismicity is geographically uniformly distributed along the Princes Islands (PI) segment. It spreads within a narrow depth range between 8 and 14km except at both ends of this basin where the seismicity extends vertically up to the surface as recently observed

by Bohnhoff et al, 2013. To the west, the extended seismic cluster corresponds to the kink of the MMF where its strike exhibits a significant change from a NW-SE to a E-W. In the eastern Marmara, the seismic cluster is located in the Tuzla region at the transition with the Izmit fault corresponding to a local complex structure. For both clusters of this segment (i.e. the kink cluster and the Tuzla cluster), the argument of Weaver (1978) about the link between fault offset and depth extension of seismic clusters is then expected to hold.

On the contrary, in the Kumburgaz basin (KB) located in the center of the Marmara Sea, seismicity is very sparse. It is of interest to see that it shares similarities with the ruptured Ganos segment (1912 earthquake) to the west and the Izmit segment (1999 earthquake) to the east where there is also very little seismicity.

2.3 SEISMOTECTONIC INTERPRETATION

Our detailed study of the recent seismicity along the Main Marmara Fault provides new constraints on the degree of coupling on segments of the fault system in the Sea of Marmara. The major result is that the Central basin (CeB) segment behaves very differently from the rest of the MMF. The seismogenic depth ds ~ 13km defined from the 90% of the cumulative depth distribution, is much deeper than the geodetic locking depth dg ~ 0-3km. In other words, most of the seismicity is taking place below the locking depth and above the ductile root of the fault. This is very different from the Cinarcik basin (CB) where $d_s \sim d_g$. The b-value of the Gutenberg-Richter distribution in CeB is significantly lower than the b-value of CB to the east (respectively 0.9 and 1.2). This b-value contrast can be related to Amistrano's results (2003) suggesting that the fault rheology is rather ductile to the west and brittle in the eastern MMF. Moreover, the seismic slip rate estimated from the cumulative seismic moment is more than two orders of magnitude larger in CeB than in the Kumburgaz segment (KB). As proposed by Wdowinski (2009), a high seismic slip rate in a domain below the locking depth is the signature of creep on the fault. Following all these arguments, the Central basin has all the indirect evidences of a domain where aseismic slip is significant. If so, it continuously relaxes significant shear stress without major seismic events (M>5). Figure 8 summarizes our interpretation of the present behavior of the different basins of the MMF.

Our observations show also that the low level of seismicity on the Kumburgaz segment at the center of the MMF is being well resolved (comparison above the completeness magnitude). The seismicity rate there is far below the rate of west Marmara (CeB and TB). This segment exhibits a fully locked behavior similar to the Ganos segment which hosted the 1912 earthquake. In the Cinarcik basin, the situation looks intermediate with seismicity mostly at the geodetic locking depth of about 10km.

The Main Marmara Fault is a major seismic gap. In this context, the estimate of the locked segment area provides an estimate of the magnitude of the main forthcoming event assuming that the rupture will not enter significantly within creeping domains. With a length of 45km and a seismogenic zone of 12km for the locked zone, a shear modulus of 35GPa, a tectonic velocity of 23mm/yr and a seismic cycle of 250yr, the expected seismic moment of an event extending over the Kumburgaz segment is of

the order of 1.1 1020Nm (i.e. Mw~ 7.3). The two adjacent domains (the Central basin segment and the Princes Island segment) could be at the seat of moderate earthquakes or could rupture with the Kumburgaz segment. Moreover, the simple geometry and the very poor activity along the Kumburgaz segment are the signature of very little stress heterogeneities along the fault plane, making it a good candidate for supershear rupture. If repeating foreshocks were expected to develop, they should emerge at depth below or at the boundaries of the segment, possibly along the vertically extended deep observed swarms.

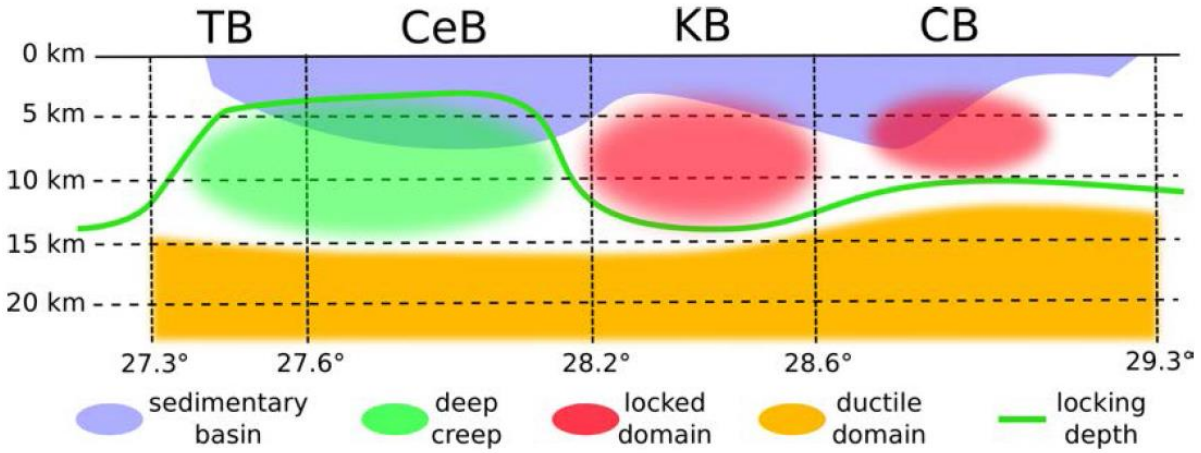

Figure 8: Interpretation of the MMF behavior: Two major asperities, a major one along the Central High and the Kumburgaz basin (KB), a secondary one in the upper part of the Cinarcik Basin (CB). The western part of the MMF including the Tekirdag basin (TB) and the Central Basin (CeB) seems to show a deep creep behavior.